Int. J. Solids Structures, 1972, Vol. 8, pp. 269 to 293. Pergamon Press. Printed in Great Britain

THE INITIATION OF COMBINED STRESS WAVES IN A THIN-WALLED TUBE DUE TO IMPACT LOADINGS

T. C. T. TING†

Department of Materials Engineering, University of Illinois at Chicago Circle, Chicago, Illinois 60680

Abstract—The solution near the impact end of a thin-walled tube is presented in which the end $x = 0$ of the pre-stressed tube is subjected to a discontinuous combined longitudinal and torsional loading at time $t = 0$. The loads at $x = 0$ after $t = 0$ are assumed to vary continuously. Solutions are obtained for all possible combinations of the discontinuous loadings at $t = 0$ and all possible variations of loads after $t = 0$. The characteristics of the solutions in each region, the initial speed and sometimes the initial acceleration of the boundary between two regions are given. These are useful guides for a complete solution of combined stress wave propagation in a thin-walled tube subjected to arbitrary impact loadings.

1. INTRODUCTION

THE unloading problem of a semi-infinite thin rod due to a longitudinal impact at the free end, $x = 0$, was studied by Rakhmatulin [1] in which the longitudinal stress σ at $x = 0$ is assumed to be increased instantaneously at time $t = 0$ to a value beyond the elastic limit and decreased gradually thereafter (see [12] for a more thorough study). For this type of impact loading, the wave pattern in the $x \sim t$ plane consists of three regions: a neutral region adjacent to the x-axis, a region of plastic waves, and an elastic unloading region adjacent to the t-axis. Moreover, in the region of plastic waves, the simple wave solution applies; i.e. the stress σ and the logitudinal particle velocity u are constant along the characteristics which are straight lines emanated from the origin $x = 0$, $t = 0$.

The problem becomes complicated if we consider combined stress waves in a thin-walled tube in which both longitudinal stress σ and torsional stress τ applied at $x = 0$ are of impact type. To illustrate the complicacy of the problem, let us consider the particular problem in which an impact type longitudinal stress alone is applied at $x = 0$ of a pre-twisted thin-walled tube. If the tube is not pre-twisted, the problem is identical to the one studied by Rakhmatulin. If the tube is pre-twisted, the wave pattern in the $x \sim t$ plane belongs to case III.4, studied in this paper (see Fig. 8). All together six regions will be generated. Moreover, the solution in the second plastic region, which would be a simple wave solution if σ at $x = 0$ were a step function, is no longer a simple wave solution.

The purpose of this paper is to study the following more general problem. The longitudinal stress σ and the torsional stress τ applied at $x = 0$ are constants for $t < 0$, have a discontinuous jump at $t = 0$ and vary continuously for $t > 0$. The variation of σ and τ for $t > 0$ at $x = 0$ can be both increasing, both decreasing, or one of them increasing while the other decreasing. The characteristics of the solution in each region are analyzed. The uniqueness and existence of the solution for each case are also discussed.

† Professor of Applied Mechanics.

The complete solution of wave propagation in the thin-walled tube for prescribed boundary values $\sigma(0, t)$ and $\tau(0, t)$ requires a numerical integration. However, before we can apply any numerical scheme to the problem, we have to know how many regions are involved near the origin $x = 0$, $t = 0$ and what are the characteristics of the solution in each region. This is a very essential step, and it is the purpose of this paper to furnish this step.

2. BASIC EQUATIONS

The governing equations for the combined longitudinal and torsional waves in a thin-walled tube of isotropic work-hardening materials are derived by Clifton [2] and can be written in the form of a matrix differential equation (see also [3]),

$$\mathbf{A}\mathbf{w}_t + \mathbf{B}\mathbf{w}_x = \mathbf{0} \tag{1}$$

where

$$\mathbf{A} = \begin{bmatrix} \rho & 0 & 0 & 0 \\ 0 & \rho & 0 & 0 \\ 0 & 0 & \dfrac{1}{E} + H\dfrac{\sigma^2}{\theta^2} & H\sigma\tau \\ 0 & 0 & H\sigma\tau & \dfrac{1}{\mu} + H\theta^2\tau^2 \end{bmatrix}$$

$$\mathbf{B} = \begin{bmatrix} 0 & 0 & -1 & 0 \\ 0 & 0 & 0 & -1 \\ -1 & 0 & 0 & 0 \\ 0 & -1 & 0 & 0 \end{bmatrix} \qquad \mathbf{w} = \begin{bmatrix} u \\ v \\ \sigma \\ \tau \end{bmatrix}$$

The subscripts t and x denote partial differentiation. u and v are the longitudinal and the circumferential particle velocities, E is Young's modulus, μ is the shear modulus and ρ is the mass density of the tube. In the elastic region $H = 0$, while in the plastic region H is a function of the yield stress k,

$$\left(\frac{\sigma}{\theta}\right)^2 + \tau^2 = k^2 \tag{2}$$

where $\theta = \sqrt{3}$ for the von-Mises yield condition and $\theta = 2$ for the Tresca yield condition.

The characteristics c of equation (1) are the roots of $|c\mathbf{A} - \mathbf{B}| = 0$. In the elastic region, the roots are $\pm c_0$ and $\pm c_2$ where $c_0^2 = E/\rho$ and $c_2^2 = \mu/\rho$. In the plastic region, the roots are denoted by $\pm c_f$ and $\pm c_s$ which stand for "fast" wave speed and "slow" wave speed respectively. It was shown in [2] that

$$0 \leq c_s \leq c_2 \leq c_f \leq c_0. \tag{3}$$

Since **A** and **B** are both symmetric in the present problem, the left eigenvector **l** and the right eigenvector **r** defined by

$$\mathbf{l}^T(c\mathbf{A}-\mathbf{B}) = \mathbf{0}, \tag{4a}$$

$$(c\mathbf{A}-\mathbf{B})\mathbf{r} = \mathbf{0}, \tag{4b}$$

are identical. If we introduce the following vectors (see [4])

$$\mathbf{f} = -\begin{bmatrix} \psi_f \\ 1 \end{bmatrix}, \qquad \mathbf{s} = \begin{bmatrix} \psi_s \\ 1 \end{bmatrix} \tag{5}$$

where

$$\psi_f = \frac{\dfrac{1}{c_2^2}-\dfrac{1}{c_f^2}}{\dfrac{1}{c_0^2}-\dfrac{1}{c_f^2}}\frac{\sigma}{\theta^2\tau} = -\frac{\dfrac{1}{c_0^2}-\dfrac{1}{c_s^2}}{\dfrac{1}{c_2^2}-\dfrac{1}{c_s^2}}\frac{\theta^2\tau}{\sigma} \tag{6a}$$

$$\psi_s = \frac{\dfrac{1}{c_2^2}-\dfrac{1}{c_s^2}}{\dfrac{1}{c_0^2}-\dfrac{1}{c_s^2}}\frac{\sigma}{\theta^2\tau} = -\frac{\dfrac{1}{c_0^2}-\dfrac{1}{c_f^2}}{\dfrac{1}{c_2^2}-\dfrac{1}{c_f^2}}\frac{\theta^2\tau}{\sigma} \tag{6b}$$

the eigenvectors **r** and **l** can be written as

$$\mathbf{r}_{f\pm} = \mathbf{l}_{f\pm} = \begin{bmatrix} \mp\mathbf{f}/\rho c_f \\ \mathbf{f} \end{bmatrix} \tag{7a}$$

$$\mathbf{r}_{s\pm} = \mathbf{l}_{s\pm} = \begin{bmatrix} \mp\mathbf{s}/\rho c_s \\ \mathbf{s} \end{bmatrix} \tag{7b}$$

where $\mathbf{r}_{f\pm}$ and $\mathbf{r}_{s\pm}$ denote the eigenvectors **r** for $c = \pm c_f$ and $c = \pm c_s$ respectively. It is shown in [2] that **f** and **s** are orthogonal to each other, i.e.

$$\mathbf{f}\cdot\mathbf{s} = 0, \quad \text{or} \quad \psi_f\psi_s = -1. \tag{8}$$

The signs for **f** and **s** in equation (5) are so chosen that they both point toward outside of the yield surface.

If $\mathrm{d}\mathbf{w}/\mathrm{d}t|_c$ denotes the total derivative of $\mathbf{w}(x, t)$ along a characteristic curve, the characteristic condition is given by (see [5, 6])

$$\mathbf{l}^T\mathbf{B}\frac{\mathrm{d}\mathbf{w}}{\mathrm{d}t}\bigg|_c = 0. \tag{9}$$

It can be shown that the eigenvectors **l** and **r** are biorthogonal to each other with respect to **B**. In particular,

$$\mathbf{l}_s^T\mathbf{B}\mathbf{r}_{s^-} = 0, \qquad \mathbf{l}_s^T\mathbf{B}\mathbf{r}_{f^+} = 0, \qquad \mathbf{l}_s^T\mathbf{B}\mathbf{r}_{f^-} = 0. \tag{10}$$

Hence along $+c_s$ characteristic curves, we obtain from equations (9) and (10) that

$$\frac{\mathrm{d}\mathbf{w}}{\mathrm{d}t}\bigg|_{c_s} = \alpha^-\mathbf{r}_{s^-} + \beta^+\mathbf{r}_{f^+} + \beta^-\mathbf{r}_{f^-} \tag{11}$$

where α^-, β^+ and β^- are scalars. One can obtain a similar equation for $\mathrm{d}\mathbf{w}/\mathrm{d}t|_{c_f}$. However, this is not needed in this paper.

Differentiation of equation (2) with respect to t yields

$$kk_t = \boldsymbol{\sigma}_t \cdot \mathbf{n} \tag{12}$$

where

$$\boldsymbol{\sigma} = \begin{bmatrix} \sigma \\ \tau \end{bmatrix}, \qquad \mathbf{n} = \begin{bmatrix} \sigma/\theta^2 \\ \tau \end{bmatrix}. \tag{13}$$

Hence $\mathbf{n}$ is the normal to the yield surface. The tangent to the yield surface will be defined by

$$\mathbf{t} = \begin{bmatrix} \theta^2\tau/\sigma \\ -1 \end{bmatrix}, \qquad \mathbf{t} \cdot \mathbf{n} = 0. \tag{14}$$

3. THE SOLUTION NEAR THE ORIGIN

We will now study the solution $\mathbf{w}(x, t)$ of equation (1) in the neighborhood of the origin $x = 0, t = 0$, when the boundary value $\mathbf{w}(0, t)$ prescribed at $x = 0$ is discontinuous at $t = 0$. To this end, let us assume that $\mathbf{w}(x, t)$ in the neighborhood of the origin can be expanded into the following series:

$$\mathbf{w}(x, t) = \mathbf{w}^{(0)}(\lambda) + t\mathbf{w}^{(1)}(\lambda) + \ldots \tag{15}$$

where

$$\lambda = x/t \tag{16}$$

and $\mathbf{w}^{(0)}$ and $\mathbf{w}^{(1)}$ are functions of λ only. Then

$$\mathbf{w}_x = \frac{1}{t}\frac{\mathrm{d}\mathbf{w}^{(0)}}{\mathrm{d}\lambda} + \frac{\mathrm{d}\mathbf{w}^{(1)}}{\mathrm{d}\lambda} + 0(t) \tag{17a}$$

$$\mathbf{w}_t = -\frac{\lambda}{t}\frac{\mathrm{d}\mathbf{w}^{(0)}}{\mathrm{d}\lambda} + \left(\mathbf{w}^{(1)} - \lambda\frac{\mathrm{d}\mathbf{w}^{(1)}}{\mathrm{d}\lambda}\right) + 0(t). \tag{17b}$$

Since $\mathbf{A}$ is a function of $\boldsymbol{\sigma}$, and hence of $\mathbf{w}$, we also have

$$\mathbf{A}(\mathbf{w}) = \mathbf{A}^{(0)} + t\mathbf{A}^{(1)} + \ldots \tag{18}$$

where

$$\mathbf{A}^{(0)} = \mathbf{A}(\mathbf{w}^{(0)}) \tag{19a}$$

$$\mathbf{A}^{(1)} = (\mathbf{w}^{(1)})^T \nabla \mathbf{A}^{(0)} \tag{19b}$$

$\nabla\mathbf{A}^{(0)}$ is the gradient of $\mathbf{A}^{(0)}$ with respect to the components of $\mathbf{w}^{(0)}$. Substitution of equations (17) and (18) into equation (1) shows that equation (1) is satisfied for all λ and t provided

$$(\lambda\mathbf{A}^{(0)} - \mathbf{B})\frac{\mathrm{d}\mathbf{w}^{(0)}}{\mathrm{d}\lambda} = \mathbf{0} \tag{20}$$

$$(\lambda\mathbf{A}^{(0)} - \mathbf{B})\frac{\mathrm{d}\mathbf{w}^{(1)}}{\mathrm{d}\lambda} = \mathbf{A}^{(0)}\mathbf{w}^{(1)} - \lambda\mathbf{A}^{(1)}\frac{\mathrm{d}\mathbf{w}^{(0)}}{\mathrm{d}\lambda}. \tag{21}$$

Let $c^{(0)}$ be the roots of

$$|c^{(0)}\mathbf{A}^{(0)}-\mathbf{B}| = 0. \tag{22}$$

Then the solution of equations (20) and (21) depends on whether $\lambda = c^{(0)}$ or not. We will call a region "regular" if $\lambda \neq c^{(0)}$ in the region, and "singular" if $\lambda = c^{(0)}$. We will discuss these two cases separately.

Regular region ($\lambda \neq c^{(0)}$)

When $\lambda \neq c^{(0)}$, equation (20) yields

$$\frac{d\mathbf{w}^{(0)}}{d\lambda} = \mathbf{0}, \quad \text{or} \quad \mathbf{w}^{(0)} = \text{const.} \tag{23}$$

and the solution of equation (21) can be shown to be

$$\mathbf{w}^{(1)} = -\mathbf{A}^{(0)^{-1}}(\lambda\mathbf{A}^{(0)}-\mathbf{B})\mathbf{q} = -\lambda\mathbf{q}+\mathbf{A}^{(0)^{-1}}\mathbf{B}\mathbf{q} \tag{24}$$

where $\mathbf{q}$ is a constant vector. Thus $\mathbf{w}^{(1)}$ depends on λ linearly. On the other hand, substitution of equations (23) and (24) into equation (17b) yields

$$\mathbf{w}_t|_{t=0} = \mathbf{A}^{(0)^{-1}}\mathbf{B}\mathbf{q} \tag{25}$$

where $t = 0$ means $t = 0^+$. Hence $\mathbf{w}_t|_{t=0}$ is a constant, independent of λ. If we eliminate $\mathbf{q}$ between equations (24) and (25), we obtain

$$(\lambda\mathbf{A}^{(0)}-\mathbf{B})\mathbf{w}_t|_{t=0} = -\mathbf{B}\mathbf{w}^{(1)}. \tag{26}$$

This is a useful relation which enables one to convert $\mathbf{w}^{(1)}$ to $\mathbf{w}_t|_{t=0}$ and vice versa within the regular region.

Singular region ($\lambda = c^{(0)}$)

When $\lambda = c^{(0)}$, equation (20) yields

$$\frac{d\mathbf{w}^{(0)}}{d\lambda} = -\zeta\mathbf{r}^{(0)} \tag{27}$$

where

$$(c^{(0)}\mathbf{A}^{(0)}-\mathbf{B})\mathbf{r}^{(0)} = \mathbf{0} \tag{28}$$

and ζ is a proportional factor which depends on λ. The negative sign is added to make ζ positive. A means of determining ζ will be given later. With equations (27) and (19b), equation (21) is a homogeneous differential equation for $\mathbf{w}^{(1)}$ which can be integrated numerically. It should be noticed, however, that the coefficient matrix of $d\mathbf{w}^{(1)}/d\lambda$ in equation (21) is singular. This poses some problems in integrating this equation for $\mathbf{w}^{(1)}$. This will be taken up again in Section 5.

For a given boundary value $\mathbf{w}(0, t)$ which is discontinuous at $t = 0$, the solution in the neighborhood of the origin consists of several sectors of "regular regions" and "singular regions". The solution $\mathbf{w}^{(0)}$ depends only on the discontinuity in the boundary values $\mathbf{w}(0, t)$ at $t = 0$. In fact $\mathbf{w}^{(0)}$ is nothing but the simple wave solution obtained in [2]. As to $\mathbf{w}^{(1)}$, the solution is obtained by equation (24) for regular regions and by integrating equation (21) for singular regions. For a step-load condition, $\mathbf{w}^{(1)} \equiv 0$ in all regions. It should

be noticed that $\mathbf{w}^{(1)}(\lambda)$ is not necessarily continuous across the boundary between a regular region and a singular region even though $\mathbf{w}(x, t)$ is required to be continuous across such a boundary. This is discussed in the next section.

4. THE CONTINUITY CONDITION

Let us consider $\mathbf{w}(x, t)$ along a curve Γ given by

$$x = \lambda_\Gamma t + \tfrac{1}{2}\kappa_\Gamma t^2 + \dots \tag{29}$$

where λ_Γ and κ_Γ are constants. In the $x \sim t$ plane, κ_Γ stands for the curvature of the curve Γ at $t = 0$. If Γ is the boundary between an elastic region and a plastic region, κ_Γ is identified as the "initial acceleration" of this boundary. Now, from equation (16), we obtain

$$\lambda = \frac{x}{t} = \lambda_\Gamma + \tfrac{1}{2}\kappa_\Gamma t + \dots$$

and substitution of λ so obtained in equation (15) yields

$$\mathbf{w}(x, t)|_{(x,t)\,\text{on}\,\Gamma} = \mathbf{w}^{(0)}(\lambda_\Gamma) + t\left\{\mathbf{w}^{(1)}(\lambda) + \frac{1}{2}\kappa_\Gamma \frac{\mathrm{d}\mathbf{w}^{(0)}}{\mathrm{d}\lambda}\right\}_{\lambda=\lambda_\Gamma} + 0(t^2). \tag{30}$$

Hence, we arrive at the result that if $\mathbf{w}(x, t)$ is continuous across Γ, $\mathbf{w}^{(0)}(\lambda)$ and $\{\mathbf{w}^{(1)}(\lambda) + \frac{1}{2}\kappa_\Gamma(\mathrm{d}\mathbf{w}^{(0)}/\mathrm{d}\lambda)\}$ must be continuous across $\lambda = \lambda_\Gamma$. The quantity in $\{\ \}$ is the total derivative of $\mathbf{w}(x, t)$ along the curve Γ evaluated at $t = 0$. Hence,

$$\lim_{t\to 0} \frac{\mathrm{d}\mathbf{w}}{\mathrm{d}t}\bigg|_\Gamma = \left\{\mathbf{w}^{(1)} + \frac{1}{2}\kappa_\Gamma \frac{\mathrm{d}\mathbf{w}^{(0)}}{\mathrm{d}\lambda}\right\}_{\lambda=\lambda_\Gamma}. \tag{31}$$

Therefore, $\lim_{t\to 0}(\mathrm{d}\mathbf{w}/\mathrm{d}t)|_\Gamma$ is continuous across Γ while $\mathbf{w}^{(1)}$ need not be continuous.

If Γ is the boundary between two regular regions, then $\mathbf{w}^{(1)}$ is continuous across Γ because $\mathrm{d}\mathbf{w}^{(0)}/\mathrm{d}\lambda = 0$ by equation (23).

If Γ is the boundary between a regular region and a singular region, then at $\lambda = \lambda_\Gamma$,

$$\{\mathbf{w}^{(1)}\}_{\text{regular region}} = \{\mathbf{w}^{(1)} - \tfrac{1}{2}\kappa_\Gamma \zeta \mathbf{r}^{(0)}\}_{\text{singular region}} \tag{32}$$

where use has been made of equations (23) and (27). If we convert $\mathbf{w}^{(1)}$ in the regular region into $\mathbf{w}_t|_{t=0}$ by using equation (26), we obtain

$$(\lambda_\Gamma \mathbf{A}^{(0)} - \mathbf{B})\mathbf{w}_t|_{t=0} = -\mathbf{B}\{\mathbf{w}^{(1)} - \tfrac{1}{2}\kappa_\Gamma \zeta \mathbf{r}^{(0)}\}_{\lambda=\lambda_\Gamma}. \tag{33}$$

It is understood that $\mathbf{w}^{(1)}$ in the right hand side is evaluated in the singular region. Equation (33) is a useful relation which will be used to convert $\mathbf{w}_t|_{t=0}$ in the regular region to $\mathbf{w}^{(0)}(\lambda_\Gamma)$ in the singular region. It should be pointed out that if the regular region adjacent to the singular region is a plastic region, then the boundary Γ is necessarily a characteristic curve because the singular region is always a plastic region. If the regular region is an elastic region, then Γ is a loading, or an unloading, boundary depending on whether $k_t > 0$ or $k_t < 0$ in the regular region.

5. THE SOLUTION IN THE SINGULAR REGION

In the singular region, $\mathbf{w}^{(0)}$ is obtained by integrating equation (27) while $\mathbf{w}^{(1)}$ is obtained by integrating equation (21). $\mathbf{w}^{(0)}$ so obtained, and in particular $\boldsymbol{\sigma}^{(0)}$, is the simple wave solution discussed in [2]. We will now discuss the solution $\mathbf{w}^{(1)}$.

If the curve Γ discussed in the previous section is one of the characteristics, equation (31) with the use of equation (27) can be written as

$$\lim_{t\to 0}\left.\frac{\mathrm{d}\mathbf{w}}{\mathrm{d}t}\right|_c = \{\mathbf{w}^{(1)} - \tfrac{1}{2}\kappa_c\zeta\mathbf{r}^{(0)}\}_{\lambda=c^{(0)}}. \tag{34}$$

The characteristic condition, equation (9), evaluated at $t = 0$ is reduced to

$$\mathbf{l}^{(0)T}\mathbf{B}(\mathbf{w}^{(1)} - \tfrac{1}{2}\kappa_c\zeta\mathbf{r}^{(0)}) = 0 \tag{35}$$

where

$$\mathbf{l}^{(0)T}(c^{(0)}\mathbf{A}^{(0)} - \mathbf{B}) = \mathbf{0}. \tag{36}$$

Consider the characteristics c in a singular region near the origin $x = 0$, $t = 0$. Since c is a function of $\boldsymbol{\sigma}$, and hence of $\mathbf{w}$, we have, using equation (15),

$$\begin{aligned} c(\mathbf{w}) &= c(\mathbf{w}^{(0)} + t\mathbf{w}^{(1)} + \ldots) \\ &= c^{(0)}(\lambda) + tc^{(1)}(\lambda) + 0(t^2) \end{aligned} \tag{37}$$

where

$$c^{(0)}(\lambda) = c(\mathbf{w}^{(0)}) = c(\boldsymbol{\sigma}^{(0)}) \tag{38a}$$

$$c^{(1)}(\lambda) = \mathbf{w}^{(1)} \cdot \nabla c^{(0)} = \boldsymbol{\sigma}^{(1)} \cdot \nabla c^{(0)}. \tag{38b}$$

Clearly, the first $\nabla c^{(0)}$ in equation (38b) is the gradient of $c^{(0)}$ with respect to the components of $\mathbf{w}^{(0)}$ while the second $\nabla c^{(0)}$ is the gradient of $c^{(0)}$ with respect to the components of $\boldsymbol{\sigma}^{(0)}$. On the other hand, if the equation of the characteristic curves emanated from the origin is expressed by the one-parameter family of equation:

$$x = \lambda_c t + \tfrac{1}{2}\kappa_c(\lambda_c)t^2 + \ldots$$

where λ_c is the parameter and κ_c depends on λ_c, we have:

$$c = \frac{\mathrm{d}x}{\mathrm{d}t} = \lambda_c + \kappa_c(\lambda_c)t + \ldots$$

$$\lambda = \frac{x}{t} = \lambda_c + \tfrac{1}{2}\kappa_c(\lambda_c)t + \ldots .$$

Elimination of the parameter λ_c between these two equations yields

$$c = \lambda + \tfrac{1}{2}\kappa_c(\lambda)t + 0(t^2). \tag{39}$$

Comparing this equation with equation (37), we obtain

$$c^{(0)}(\lambda) = c(\boldsymbol{\sigma}^{(0)}) = c(\mathbf{w}^{(0)}) = \lambda \tag{40a}$$

$$c^{(1)}(\lambda) = \tfrac{1}{2}\kappa_c(\lambda) = \boldsymbol{\sigma}^{(1)} \cdot \nabla c^{(0)} \tag{40b}$$

by equation (38). Therefore κ_c, the curvature of the characteristics at $t = 0$, can be determined by equation (40b).

Since $\mathbf{w}^{(0)}$ is a function of λ, differentiation of equation (40a) with respect to λ yields

$$\nabla c^{(0)} \cdot \frac{d\mathbf{w}^{(0)}}{d\lambda} = 1, \tag{41a}$$

or by equation (27),

$$-\zeta \mathbf{r}^{(0)} \cdot \nabla c^{(0)} = 1. \tag{41b}$$

Equation (41b) furnishes a means of determining $\zeta(\lambda)$. In particular, when $c^{(0)} = c_s^{(0)}$, we have, using equation (7b),

$$-\zeta \mathbf{s}^{(0)} \cdot \nabla c_s^{(0)} = 1. \tag{41c}$$

The left eigenvector $\mathbf{l}$ defined by equation (4a) is a function of $\mathbf{w}$. Using equation (15) for $\mathbf{w}$, we write

$$\mathbf{l}(\mathbf{w}) = \mathbf{l}^{(0)}(\lambda) + t\mathbf{l}^{(1)}(\lambda) + 0(t^2) \tag{42}$$

where

$$\mathbf{l}^{(0)}(\lambda) = \mathbf{l}(\mathbf{w}^{(0)}) \tag{43a}$$

$$\mathbf{l}^{(1)}(\lambda) = \mathbf{w}^{(1)T} \nabla \mathbf{l}^{(0)}. \tag{43b}$$

If we substitute equations (42), (39) and (18) into equation (4a), we obtain equation (36) and

$$\mathbf{l}^{(1)T}(\lambda \mathbf{A}^{(0)} - \mathbf{B}) + \mathbf{l}^{(0)T}(\tfrac{1}{2}\kappa_c \mathbf{A}^{(0)} + \lambda \mathbf{A}^{(1)}) = \mathbf{0}. \tag{44}$$

If we post-multiply equation (44) by $\mathbf{r}^{(0)}$, the first term vanishes in view of equation (28). Hence

$$\mathbf{l}^{(0)T}(\tfrac{1}{2}\kappa_c \mathbf{A}^{(0)} + \lambda \mathbf{A}^{(1)})\mathbf{r}^{(0)} = 0,$$

or, using equations (36) and (40a),

$$\frac{1}{2\lambda}\kappa_c \mathbf{l}^{(0)T} \mathbf{B} \mathbf{r}^{(0)} + \lambda \mathbf{l}^{(0)T} \mathbf{A}^{(1)} \mathbf{r}^{(0)} = 0. \tag{45}$$

Equations (45), (35) and (27) assure that the right hand side of equation (21) is orthogonal to $\mathbf{l}^{(0)}$; a condition necessary for the existence of a solution for $d\mathbf{w}^{(1)}/d\lambda$ from equation (21) (see [7]). Equation (21) can now be solved for $d\mathbf{w}^{(1)}/d\lambda$ and the resulting equation integrated for $\mathbf{w}^{(1)}$ numerically. Although $d\mathbf{w}^{(1)}/d\lambda$ obtained from equation (21) is not unique and involves an arbitrary factor, this arbitrary factor can be fixed by using equation (35). Thus $d\mathbf{w}^{(1)}/d\lambda$ has a unique solution in terms of $\mathbf{w}^{(0)}$ and $\mathbf{w}^{(1)}$, and a step by step numerical integration can be employed to determine $\mathbf{w}^{(1)}$.

For the purpose of this paper, however, it is more convenient to express $\mathbf{w}^{(1)}$ in terms of the right eigenvectors $\mathbf{r}$. We will consider the case $c^{(0)} = c_s^{(0)}$. Then from equations (11) and (34), $\mathbf{w}^{(1)}$ must have the form

$$\mathbf{w}^{(1)}(\lambda) = \tfrac{1}{2}\kappa_c \zeta \mathbf{r}_{s^+}^{(0)} + \alpha^-(\lambda)\mathbf{r}_{s^-}^{(0)} + \beta^+(\lambda)\mathbf{r}_{f^+}^{(0)} + \beta^-(\lambda)\mathbf{r}_{f^-}^{(0)} \tag{46}$$

in the region where $c^{(0)} = c_s^{(0)}$. α^-, β^+ and β^- are scalar functions of λ. κ_c is, by equation (40b), related to $\sigma^{(1)}$ and hence to $\mathbf{w}^{(1)}$. In fact κ_c can be expressed in terms of α^-, β^+ and

β^- as in the following. Equation (46) is equivalent to four scalar equations. The last two equations can be written as, using equation (7),

$$\boldsymbol{\sigma}^{(1)}(\lambda) = (\tfrac{1}{2}\kappa_c\zeta + \alpha^-)\mathbf{s}^{(0)} + (\beta^+ + \beta^-)f^{(0)}.$$

If we multiply both sides of this equation by $\nabla c_s^{(0)}$ and make use of equations (40b) and (41c), we obtain

$$\kappa_c = \alpha^- \mathbf{s}^{(0)} \cdot \nabla c_s^{(0)} + (\beta^+ + \beta^-)\mathbf{f}^{(0)} \cdot \nabla c_s^{(0)}. \tag{47}$$

Therefore in the region $c^{(0)} = c_s^{(0)}$, $\mathbf{w}^{(1)}(\lambda)$ is completely characterized by three scalar functions $\alpha^-(\lambda)$, $\beta^+(\lambda)$ and $\beta^-(\lambda)$. If we eliminate κ_c between equations (46) and (47), and substitute the resulting equation in equation (21), we obtain a system of first order differential equations for α^-, β^+ and β^- which can be integrated numerically. Once we obtain α^-, β^+ and β^-, $\mathbf{w}^{(1)}$ is obtained from equations (46) and (47).

6. IMPACT ON A THIN-WALLED TUBE

We will use the results obtained in the previous sections to study the solutions $\mathbf{w}(x, t)$ near the origin $x = 0, t = 0$, when the boundary condition $\mathbf{w}(0, t)$ is discontinuous at $t = 0$. Actually, only $\boldsymbol{\sigma}(0, t)$ is assumed to be prescribed. For simplicity we will drop the superscript (0) but retain the superscript (1). On the other hand, the superscripts e and p stand for the elastic and plastic regions, respectively. Superscripts other than e and p, such as a, b or m, denote the limiting value of the quantity in the region a, b or m as (x, t) approaches the origin (see Fig. 1). In particular, if $\varepsilon > 0$,

$$\boldsymbol{\sigma}^a = \lim_{\varepsilon \to 0} \boldsymbol{\sigma}(0, \varepsilon)$$

$$\boldsymbol{\sigma}^b = \lim_{\varepsilon \to 0} \boldsymbol{\sigma}(0, -\varepsilon).$$

Thus $\boldsymbol{\sigma}^b$ and $\boldsymbol{\sigma}^a$ are the stress states at $x = 0$, just "before" and "after" $t = 0$, respectively. We will assume that $\boldsymbol{\sigma}(x, t) \equiv \boldsymbol{\sigma}^b$ for $x > 0$, $t < 0$; i.e. the tube is initially prestressed to the constant stress $\boldsymbol{\sigma}^b$. Then $\boldsymbol{\sigma}(x, t) \equiv \boldsymbol{\sigma}^b$ also for $x - c_0 t > 0$, or $x - c_f^b t > 0$ depending on the situation, and the region b is a "neutral" state which is denoted by N. Moreover, we assume that $\boldsymbol{\sigma}^b$ is beyond the elastic limit and hence is on a yield surface. The case when $\boldsymbol{\sigma}^b$ is below the initial yield surface requires only a simple modification and hence the assumption does not lose the generality of the results obtained here.

Now, depending on the relative position of $\boldsymbol{\sigma}^b$ and $\boldsymbol{\sigma}^a$ in the $\sigma \sim \tau$ plane, the problem can be divided into several groups. Within each group, there may be up to four different cases depending on the direction of $\boldsymbol{\sigma}_t^a$, which is the direction of the stress path $\boldsymbol{\sigma}(0, t)$ in the $\sigma \sim \tau$ plane right after $t = 0$. In this paper we will restrict both $\boldsymbol{\sigma}^b$ and $\boldsymbol{\sigma}^a$ to be in the first quadrant of the $\sigma \sim \tau$ plane. Then there are six groups which exhaust all possibilities. The first two groups are actually special cases of other groups, but since the results are not easily reducible, and moreover some properties are not readily visible from other groups, they are presented as separate groups. As a matter of fact, presentation of groups I and II simplifies the analysis of the rest of the groups.

Group I

In this group, $\boldsymbol{\sigma}^a$ is on the stress path for fast simple waves leading from $\boldsymbol{\sigma}^b$ (see Figs. 1–4). Depending on the direction of $\boldsymbol{\sigma}_t^a$, there are four cases which we will discuss separately below.

Case I.1. If the vector $\boldsymbol{\sigma}_t^a$ is between **s** and **t**, the wave pattern in the $x \sim t$ plane will have the form shown in Fig. 1. N stands for the neutral region and P for the plastic region. According to Lax [8], *the solution in a region which is adjacent to a constant region is a*

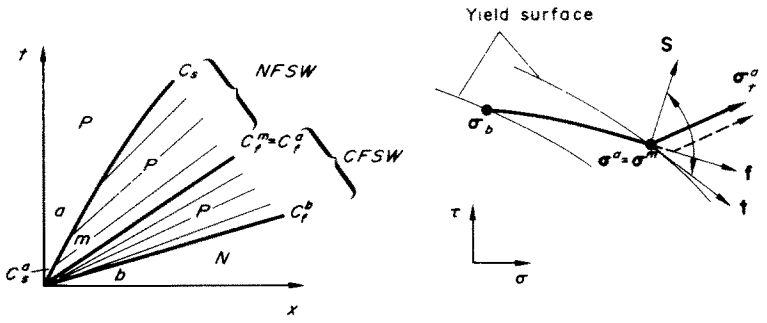

CFSW= centered fast simple waves
NFSW= non centered fast simple waves

FIG. 1. Case I.1.

simple wave solution. Thus in the region next to N bounded by c_f^b and c_f^a we have "centered fast simple waves" and abbreviated by *CFSW*. Actually, Lax's theorem can be generalized as follows: *if a region is bounded by a characteristic and* **w** *is constant on this characteristic, then the solution in the region is a simple wave solution.* The proof is omitted here. Using this general result, we see that the solution in the region m bounded by c_s and c_f^a must be a simple wave solution since **w** is constant on c_f^a. This time, however, the solution is "non-centered fast simple waves" and abbreviated by *NFSW*. Therefore,

$$\boldsymbol{\sigma}_t^m = \gamma \mathbf{f}^a \tag{48}$$

where γ is a constant. Since the discontinuity in $\boldsymbol{\sigma}_t$ across c_s^a is proportional to $\mathbf{s}^a$ (see [4]), we have

$$\boldsymbol{\sigma}_t^m - \boldsymbol{\sigma}_t^a = \eta \mathbf{s}^a \tag{49}$$

where η is a constant.

From the orthogonality condition $\mathbf{f} \cdot \mathbf{s} = 0$, we obtain from equations (48) and (49)

$$\gamma = (\boldsymbol{\sigma}_t^a \cdot \mathbf{f}^a)/(\mathbf{f}^a \cdot \mathbf{f}^a). \tag{50}$$

Thus $\gamma > 0$ which assures that $\boldsymbol{\sigma}_t^m$ as expressed by equation (48) points towards outside of the yield surface and hence region m is indeed plastic.

The dotted line in the $\sigma \sim \tau$ plane shows qualitatively how the stress state of a fixed station $x \neq 0$ will vary as time t increases.

Case I.2. For this case, Fig. 2, $\boldsymbol{\sigma}_t^a$ is between **t** and the vertical line drawn downward from $\boldsymbol{\sigma}^a$. Mathematically, this condition is given by

$$k_t^a < 0, \qquad \sigma_t^a > 0. \tag{51}$$

As in case I.1, we have *CFSW* followed by *NFSW*. Thus equation (48) still applies. Using equation (5), we write

$$\sigma_t^m = \psi_f^m \tau_t^m. \tag{52}$$

In Fig. 2, E stands for the elastic region. The discontinuity in $\boldsymbol{\sigma}_t$ across the unloading boundary c_u is given by (see [9, 4]),

$$\sigma_t^a - \sigma_t^m = G(c_0, c_2, c_u)\frac{\theta^2}{\sigma^a}k^a k_t^a \tag{53}$$

$$\tau_t^a - \tau_t^m = G(c_2, c_0, c_u)\frac{1}{\tau^a}k^a k_t^a \tag{54}$$

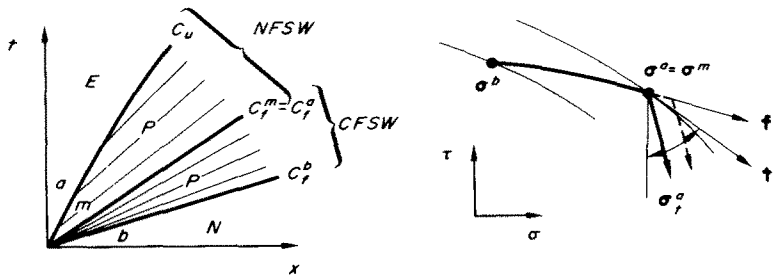

FIG. 2. Case I.2.

where

$$G(c_0, c_2, c_u) = \frac{\left(\frac{1}{c_0^2}-\frac{1}{c_f^2}\right)\left(\frac{1}{c_0^2}-\frac{1}{c_s^2}\right)\left(\frac{1}{c_2^2}-\frac{1}{c_u^2}\right)}{\left(\frac{1}{c_u^2}-\frac{1}{c_f^2}\right)\left(\frac{1}{c_u^2}-\frac{1}{c_s^2}\right)\left(\frac{1}{c_2^2}-\frac{1}{c_0^2}\right)}.$$

Elimination of σ_t^m, τ_t^m between equations (52)–(54) yields the following equation for c_u:

$$\frac{\left(\frac{1}{c_u^2}-\frac{1}{c_2^2}\right)\left(\frac{1}{c_s^2}-\frac{1}{c_0^2}\right)}{\left(\frac{1}{c_s^2}-\frac{1}{c_u^2}\right)\left(\frac{1}{c_2^2}-\frac{1}{c_0^2}\right)} = -\frac{\sigma^a\sigma_t^a}{\theta^2 k^a k_t^a} \tag{55}$$

where c_s should be c_s^a. In view of equation (51), it is not difficult to show that there exists one and only one c_u in the range $c_s^a \le c_u \le c_2$.

Again, the dotted line in the $\sigma \sim \tau$ plane shows qualitatively the stress path of other stations $x \neq 0$, as t increases.

Case I.3. This case applies when $\boldsymbol{\sigma}_t^a$ is between $\mathbf{s}$ and $-\mathbf{t}$ (Fig. 3). The boundary between the region m and the region of $CFSW$ is an unloading boundary across which equation (33) applies. Writing in terms of the present case, we have

$$(c_f^a\mathbf{A}^e - \mathbf{B})\mathbf{w}_t^m = \tfrac{1}{2}\kappa_\Gamma\zeta\mathbf{B}\mathbf{r}_f^m, \tag{56}$$

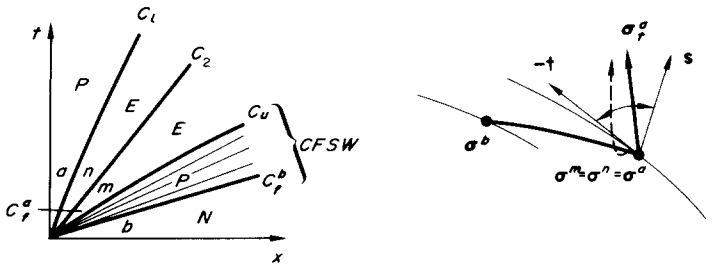

FIG. 3. Case I.3.

since $\mathbf{w}^{(1)} \equiv 0$ in the *CFSW* region and the region m is elastic. If we solve for $\mathbf{w}_t^m$ we have

$$\mathbf{w}_t^m = \frac{\kappa_\Gamma(c_f)\zeta(c_f)}{\left(\frac{c_f^2}{c_2^2}-1\right)} \begin{bmatrix} \psi_f^2 \dfrac{\theta^2\tau}{\sigma}\left(\dfrac{c_f^2}{c_0^2}+1\right)\dfrac{1}{2\rho c_f} \\ \left(\dfrac{c_f^2}{c_2^2}+1\right)\dfrac{1}{2\rho c_f} \\ -\psi_f^2\dfrac{\theta^2\tau}{\sigma} \\ -1 \end{bmatrix} \tag{57}$$

where c_f, ψ_f, σ and τ in the right hand side should be c_f^m, ψ_f^m, σ^m and τ^m. In this case, c_f^m, ψ_f^m, σ^m and τ^m are identical to c_f^a, ψ_f^a, σ^a and τ^a, respectively.

The last two components of equation (57) imply that

$$\sigma_t^m = \frac{\theta^2\tau^a}{\sigma^a}(\psi_f^a)^2\tau_t^m. \tag{58}$$

The discontinuity across the loading boundary c_l is (see [9])

$$\left(\frac{1}{c_0^2}-\frac{1}{c_l^2}\right)(\sigma_t^n-\sigma_t^a) = \rho H\sigma^a k^a k_t^a \tag{59}$$

$$\left(\frac{1}{c_2^2}-\frac{1}{c_l^2}\right)(\tau_t^n-\tau_t^a) = \rho H\theta^2\tau^a k^a k_t^a. \tag{60}$$

The condition across c_2 is

$$\sigma_t^m = \sigma_t^n. \tag{61}$$

Finally, the fact that the yield stress k on c_l and c_u must be identical for each x means that (see [4])

$$k_t^m\left(\frac{1}{c_2}-\frac{1}{c_f^a}\right)+k_t^n\left(\frac{1}{c_l}-\frac{1}{c_2}\right) = 0. \tag{62}$$

Omitting the lengthy algebraic manipulations, equations (58)–(62) can be reduced to the following single equation for c_l:

$$\frac{\left(\frac{1}{c_l^2}-\frac{1}{c_s^2}\right)}{\left(\frac{1}{c_l^2}-\frac{1}{c_0^2}\right)}\left\{1+\frac{\left(\frac{1}{c_f}+\frac{1}{c_2}\right)\left(\frac{1}{c_l^2}-\frac{1}{c_f^2}\right)\left(\frac{1}{c_s^2}-\frac{1}{c_0^2}\right)}{\left(\frac{1}{c_l}+\frac{1}{c_2}\right)\left(\frac{1}{c_s^2}-\frac{1}{c_f^2}\right)\left(\frac{1}{c_f^2}-\frac{1}{c_0^2}\right)}\right\}k^a k_t^a = -(\boldsymbol{\sigma}_t^a \cdot \mathbf{f}^a)\tau^a \tag{63}$$

c_f and c_s in this equation are actually c_f^a and c_s^a. c_l obtained from this equation is the "initial" speed of the loading boundary between the regions n and a. Again it can be shown that for $0 \le c_l \le c_s^a$, there exists only one solution.

Case I.4. The conditions on $\boldsymbol{\sigma}_t^a$ for this case to apply are (see Fig. 4)

$$k_t^a \le 0, \qquad \sigma_t^a \le 0. \tag{64}$$

Equation (58) still applies to $\boldsymbol{\sigma}_t^m$, and since $\sigma_t^m = \sigma_t^a$, we have

$$\boldsymbol{\sigma}_t^m = \sigma_t^a \begin{bmatrix} 1 \\ \dfrac{\sigma^a}{\theta^2 \tau^a}(\psi_s^a)^2 \end{bmatrix}. \tag{65}$$

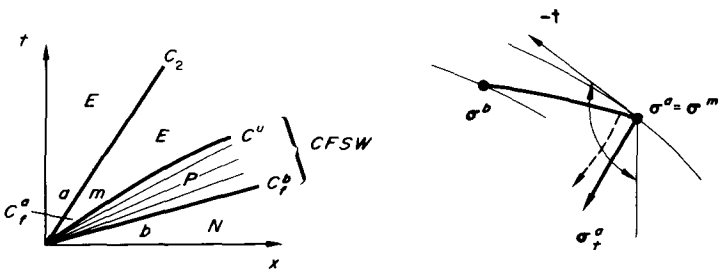

FIG. 4. Case I.4.

It should be noticed that the "entire" unloading boundary c_u and the solution in the region bounded by c_2 and c_u are determined by the boundary value $\sigma(0, t)$ alone and are independent of $\tau(0, t)$.

Group II

In this group $\boldsymbol{\sigma}^a$ is on the stress path for slow simple waves leading from $\boldsymbol{\sigma}^b$ (Figs. 5 and 6). There are four cases depending on the direction of $\boldsymbol{\sigma}_t^a$.

Case II.1. This case applies when $\boldsymbol{\sigma}_t^a$ is bounded by **s** and **t** (Fig. 5). The region m is a region of *NFSW*. Hence

$$\mathbf{w}_t^m = \gamma \mathbf{r}_f^b \tag{66}$$

where γ is a constant to be determined. The condition across c_s^b can be obtained by using equation (33):

$$(c_s^b \mathbf{A}^m - \mathbf{B})\mathbf{w}_t^m = -B\{\mathbf{w}^{(1)}(c_s^b) - \tfrac{1}{2}\kappa_c(c_s^b)\zeta(c_s^b)\mathbf{r}_s^b\}.$$

Substitution of $\mathbf{w}_t^m$ from equation (66) yields

$$\mathbf{w}^{(1)}(c_s^b) = \tfrac{1}{2}\kappa_c(c_s^b)\zeta(c_s^b)\mathbf{r}_s^b + \gamma\left(1 - \frac{c_s^b}{c_f^b}\right)\mathbf{r}_f^b.$$

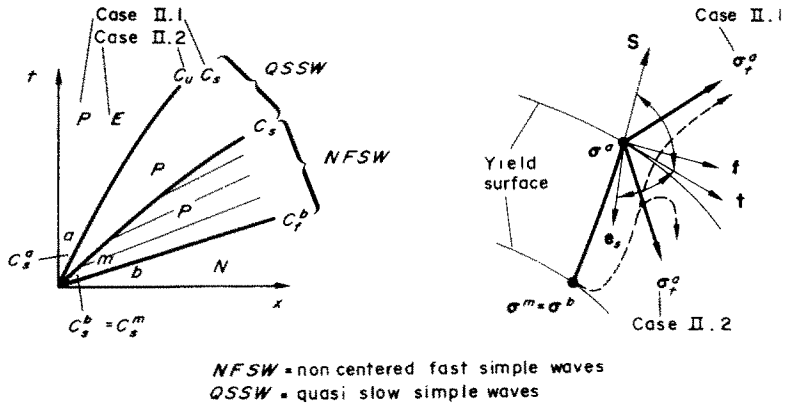

FIG. 5. Cases II.1 and II.2.

Comparing this with equation (46), it is seen that

$$\alpha^-(\lambda) = \beta^-(\lambda) = 0, \qquad \beta^+(\lambda) = \gamma\left(1 - \frac{c_s^b}{c_f^b}\right), \quad \text{for} \quad \lambda = c_s^b. \tag{67}$$

With this as the initial condition, one can integrate equation (21) to obtain $\mathbf{w}^{(1)}(\lambda)$ for $c_s^b \geq \lambda \geq c_s^a$. This applies to the singular region which is between the regions a and m. This region is called "quasi-slow simple waves" and abbreviated by $QSSW$ because if $\mathbf{w}^{(1)}$ were identically zero, the region would be a slow simple wave region.

In using equations (67) as the initial condition, γ is still an unknown quantity. However, since equation (21) is linear in $\mathbf{w}^{(1)}$, if $\bar{\mathbf{w}}^{(1)}(\lambda)$ is the solution with $\gamma = 1$, the actual solution is $\mathbf{w}^{(1)} = \gamma\bar{\mathbf{w}}^{(1)}(\lambda)$. Thus despite the fact that γ is an unknown, the numerical integration for $\mathbf{w}^{(1)}(\lambda)$ with the initial condition equation (67) can be carried out by using the particular solution for $\gamma = 1$.

Suppose we have obtained the solution $\mathbf{w}^{(1)}(\lambda)$. This means we have obtained $\alpha^-(\lambda)$, $\beta^+(\lambda)$ and $\beta^-(\lambda)$ for $c_s^b \geq \lambda \geq c_s^a$. In particular, we know $\beta^+(c_s^a)$, $\beta^-(c_s^a)$ and $\mathbf{w}^{(1)}(c_s^a)$. Now, the condition across c_s^a between the region a and the region of $QSSW$ is obtained by using equation (33).

$$\begin{aligned}(c_s^a\mathbf{A}^a - \mathbf{B})\mathbf{w}_t^a &= -\mathbf{B}\{\mathbf{w}^{(1)}(c_s^a) - \tfrac{1}{2}\kappa_c(c_s^a)\zeta(c_s^a)\mathbf{r}_s^a\} \\ &= -\mathbf{B}\{\alpha^-(c_s^a)\mathbf{r}_{s^-}^a + \beta^+(c_s^a)\mathbf{r}_{f^+}^a + \beta^-(c_s^a)\mathbf{r}_{f^-}^a\}\end{aligned} \tag{68}$$

by equation (46). If we solve this equation for $\mathbf{w}_t^a$, or for $\boldsymbol{\sigma}_t^a$ in particular, keeping in mind that the region a is plastic, we obtain

$$\boldsymbol{\sigma}_t^a = \{\delta + \tfrac{1}{2}\alpha^-(c_s^a)\}\mathbf{s}^a + \frac{\Omega^a}{1 - (c_s^a/c_f^a)^2}\mathbf{f}^a \tag{69}$$

where δ is a constant and

$$\Omega^* = \left(1 + \frac{c_s^*}{c_f^*}\right)\beta^+(c_s^*) + \left(1 - \frac{c_s^*}{c_f^*}\right)\beta^-(c_s^*). \tag{70}$$

Equation (69) is equivalent to two scalar equations for the two unknown constants δ and γ. Ω^a in equation (69) is obtained by replacing * in (70) by a.

The validity of the solution requires that $\gamma > 0$. Assuming that this is indeed the case, we have, by equations (67) and (70), $\Omega^b > 0$. If $\boldsymbol{\sigma}^a$ is not very far from $\boldsymbol{\sigma}^b$, Ω^a will also be positive and $\boldsymbol{\sigma}_t^a$ defined by equation (69) is indeed between $\mathbf{s}^a$ and $\mathbf{t}^a$ as shown in Fig. 5.

If $\boldsymbol{\sigma}^a$ is very far from $\boldsymbol{\sigma}^b$ and as a result if Ω^a is negative, then $\boldsymbol{\sigma}_t^a$ obtained by equation (69) will be between $\mathbf{s}^a$ and $-\mathbf{t}^a$. That is, the wave pattern in the $x \sim t$ plane of Fig. 5, is a result of the loading shown in the $\sigma \sim \tau$ plane of Fig. 6, in which $\boldsymbol{\sigma}_t^a$ is between $\mathbf{s}^a$ and $-\mathbf{t}^a$, (i.e. case II.3). Therefore, regardless of $\Omega^a > 0$ or $\Omega^a < 0$, there exists only one solution. However, this second solution due to $\Omega^a < 0$ is considered unlikely for the following reason. If c_s^a is so much different from c_s^b and Ω^a has to change its value from positive to negative, there exists a case in which $\Omega^a = 0$. If $\Omega^a = 0$, then $\gamma = \infty$ which is physically unrealistic.

Case II.2. This case applies when $\boldsymbol{\sigma}_t^a$ is between $\mathbf{t}$ and $\mathbf{e}_s$ as shown in Fig. 5. $\mathbf{e}_s$ will be defined later. The analysis is the same as case II.1 except that the region a is now elastic. Therefore, equation (68) is replaced by

$$\begin{aligned}(c_s^a\mathbf{A}^e - \mathbf{B})\mathbf{w}_t^a &= -\mathbf{B}\{\mathbf{w}^{(1)}(c_s^a) - \tfrac{1}{2}\kappa_\Gamma(c_s^a)\zeta(c_s^a)\mathbf{r}_{s^+}^a\} \\ &= -\mathbf{B}\{\tfrac{1}{2}[\kappa_c(c_s^a) - \kappa_\Gamma(c_s^a)]\zeta(c_s^a)\mathbf{r}_{s^+}^a + \alpha^-(c_s^a)\mathbf{r}_{s^-}^a + \beta^+(c_s^a)\mathbf{r}_{f^+}^a + \beta^-(c_s^a)\mathbf{r}_{f^-}^a\}\end{aligned}$$

by equation (46). If we solve this equation for $\mathbf{w}_t^a$, or for $\boldsymbol{\sigma}_t^a$ in particular, we obtain

$$\boldsymbol{\sigma}_t^a = \frac{1}{1-(c_s^a/c_2)^2}\{[\kappa_c(c_s^a) - \kappa_\Gamma(c_s^a)]\zeta(c_s^a)\mathbf{e}_s^a + \Omega^a\mathbf{t}^a\} \tag{71}$$

where Ω^a is defined in equation (70) and

$$\mathbf{e}_s = -\begin{bmatrix} \dfrac{\theta^2\tau}{\sigma}\psi_s^2 \\ 1 \end{bmatrix}. \tag{72}$$

It can be shown that $\mathbf{e}_s$ always lies to the right of $-\mathbf{s}$ as shown in Fig. 5. Equation (71) is equivalent to two scalar equations for the two unknowns γ and $\kappa_\Gamma(c_s^a)$, the latter is the initial acceleration of the unloading boundary c_u.

Case II.3. If $\boldsymbol{\sigma}_t^a$ is between $\mathbf{s}$ and $-\mathbf{t}$, the wave pattern in the $x \sim t$ plane will be the one shown in Fig. 6. By Lax's theorem, we have simple waves in the regions m and n. In the regions m and n, σ and u are constants along straight lines with $\mathrm{d}x/\mathrm{d}t = c_0$. Moreover, τ and v are constants along straight lines with $\mathrm{d}x/\mathrm{d}t = c_2$ in the region n. Hence, we can write

$$\mathbf{w}_t^m = \begin{bmatrix} -\sigma_t^m/\rho c_o \\ 0 \\ \sigma_t^m \\ 0 \end{bmatrix}, \qquad \mathbf{w}_t^n = \begin{bmatrix} -\sigma_t^m/\rho c_0 \\ -\sigma_t^n/\rho c_2 \\ \sigma_t^m \\ \tau_t^n \end{bmatrix}. \tag{73}$$

The fact that the yield stress k on c_l and c_0 must be the same for each x means that [4],

$$k_t^m\left(\frac{1}{c_2} - \frac{1}{c_0}\right) + k_t^n\left(\frac{1}{c_s^b} - \frac{1}{c_2}\right) = 0. \tag{74}$$

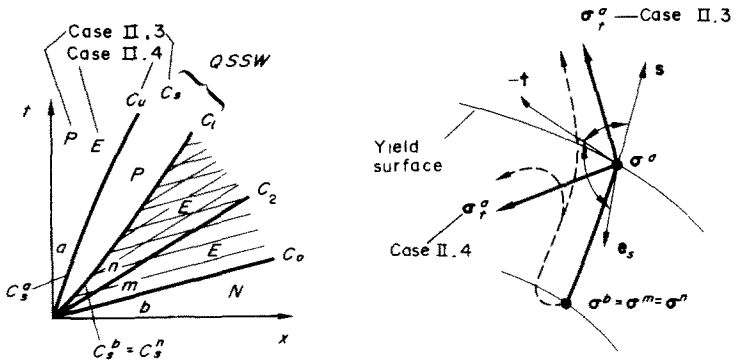

FIG. 6. Cases II.3 and II.4.

Equation (74) is reduced to, using equation (73),

$$\tau_t^n = -\frac{\left(\frac{1}{c_s^b}-\frac{1}{c_0}\right)}{\left(\frac{1}{c_s^b}-\frac{1}{c_2}\right)}\frac{\sigma^b}{\theta^2\tau^b}\sigma_t^m. \tag{75}$$

The condition across the elastic–plastic boundary c_l is obtained by using equation (33):

$$\begin{aligned}(c_s^n\mathbf{A}^e-\mathbf{B})\mathbf{w}_t^n &= -\mathbf{B}\{\mathbf{w}^{(1)}(c_s^n)-\tfrac{1}{2}\kappa_\Gamma(c_s^n)\zeta(c_s^n)\mathbf{r}_{s^+}^n\}\\ &= -\mathbf{B}\{\tfrac{1}{2}[\kappa_c(c_s^n)-\kappa_\Gamma(c_s^n)]\zeta(c_s^n)\mathbf{r}_{s^+}^n+\alpha^-(c_s^n)\mathbf{r}_{s^-}^n\\ &\quad+\beta^+(c_s^n)\mathbf{r}_{f^+}^n+\beta^-(c_s^n)\mathbf{r}_{f^-}^n\}.\end{aligned} \tag{76}$$

From equations (73), (75) and (76), we find, omitting the lengthy calculations,

$$\tfrac{1}{2}[\kappa_c(c_s^n)-\kappa_\Gamma(c_s^n)]\zeta(c_s^n) = -c_s\left(\frac{1}{c_s}+\frac{1}{c_0}\right)\left(\frac{1}{c_s}+\frac{1}{c_2}\right)\left(\frac{1}{c_2^2}-\frac{1}{c_f^2}\right)\phi \tag{77}$$

$$\alpha^-(c_s^n) = c_s\left(\frac{1}{c_s}-\frac{1}{c_0}\right)\left(\frac{1}{c_s}-\frac{1}{c_2}\right)\left(\frac{1}{c_2^2}-\frac{1}{c_f^2}\right)\phi \tag{78a}$$

$$\beta^+(c_s^n) = c_f\left(\frac{1}{c_2}+\frac{1}{c_f}\right)\left(\frac{1}{c_f}+\frac{1}{c_0}\right)\left(\frac{1}{c_s^2}-\frac{1}{c_2^2}\right)\phi \tag{78b}$$

$$\beta^-(c_s^n) = c_f\left(\frac{1}{c_2}-\frac{1}{c_f}\right)\left(\frac{1}{c_f}-\frac{1}{c_0}\right)\left(\frac{1}{c_s^2}-\frac{1}{c_0^2}\right)\phi \tag{78c}$$

where

$$\phi = \frac{\sigma^b c_s}{2\theta^2\tau^b}\frac{\left(\frac{1}{c_s}-\frac{1}{c_0}\right)\sigma_t^m}{\left(\frac{1}{c_2}+\frac{1}{c_0}\right)\left(\frac{1}{c_s^2}-\frac{1}{c_f^2}\right)} \tag{79}$$

c_s and c_f in the right hand sides of equations (77)–(79) are c_s^n and c_f^n, respectively. With the initial values of α^-, β^+ and β^- given by equations (78), $\mathbf{w}^{(1)}$ in the region of $QSSW$ can be obtained in the similar manner as in case II.1. In particular, consideration of the condition across c_s^a yields the same equation (69) from which the two unknowns δ and σ_t^m are determined. Notice that $\kappa_c(c_s^n)$, the initial curvature of the characteristic curve with initial slope c_s^n, is determined by using equation (40b) while $\kappa_\Gamma(c_s^n)$, the initial curvature of the loading boundary c_t is determined by equation (77).

The validity of the solution requires that $\sigma_t^m < 0$. Hence β^+ and β^- are negative initially by equations (78b) and (78c). By the same argument as in case II.1, Ω^a of equation (70) will be negative. Hence $\boldsymbol{\sigma}_t^a$ as expressed by equation (69) will be between $\mathbf{s}^a$ and $-\mathbf{t}^a$ as shown in Fig. 6.

Case II.4. This case applies when $\boldsymbol{\sigma}_t^a$ is between $-\mathbf{t}$ and $\mathbf{e}_s$ (Fig. 6). The analysis is exactly the same as in case II.3 except the last step, where instead of equation (69), equation (71) is used to determine σ_t^m and $\kappa_\Gamma(c_s^a)$.

Group III

In this group $\boldsymbol{\sigma}^a$ can be reached from $\boldsymbol{\sigma}^b$ by following the stress path for fast simple waves and then the stress path for slow simple waves (Figs. 7 and 8). There are four cases.

Case III.1 *and case* III.2. The solutions of these two cases (Fig. 7) can be obtained from

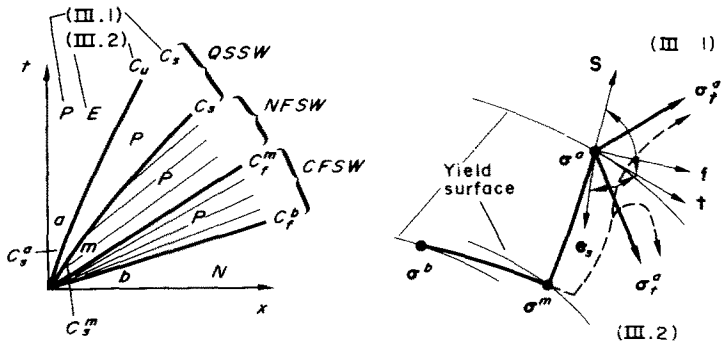

FIG. 7. Cases III.1 and III.2.

the solutions of cases II.1 and II.2 by adding an additional centered fast simple wave region.

Case III.3 *and case* III.4. For these two cases (Fig. 8), $\mathbf{w}_t^m$ is given by equation (57) while $\mathbf{w}_t^n$ can be written as

$$\mathbf{w}_t^n = \mathbf{w}_t^m + \frac{\kappa_\Gamma(c_f^m)\zeta(c_f^m)}{(c_f^m/c_2)^2 - 1} \begin{bmatrix} 0 \\ -\gamma/\rho c_2 \\ 0 \\ \gamma \end{bmatrix} \tag{80}$$

where γ is to be determined. The condition that k be identical on c_t and c_u yields [4],

$$k_t^m\left(\frac{1}{c_2} - \frac{1}{c_f^m}\right) + k_t^n\left(\frac{1}{c_s^n} - \frac{1}{c_2}\right) = 0.$$

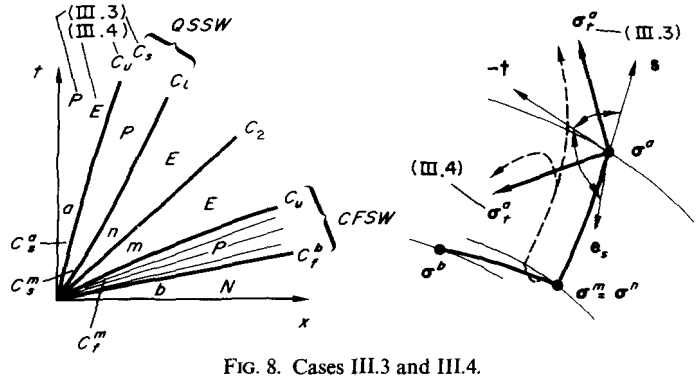

FIG. 8. Cases III.3 and III.4.

This is reduced to, using equations (57) and (80),

$$\gamma = \frac{\left(\frac{1}{c_s^m} - \frac{1}{c_f^m}\right)}{\left(\frac{1}{c_s^m} - \frac{1}{c_2}\right)}[1 + (\psi_f^m)^2] > 0. \tag{81}$$

Thus γ is determined by equation (81). The condition across the loading boundary c_l is the same equation obtained in equation (76). Substitution of $\mathbf{w}_i^n$ from equation (80) with γ expressed by equation (81) into (76), we find, omitting the extremely lengthy calculations:

$$\tfrac{1}{2}[\kappa_c(c_s^n) - \kappa_\Gamma(c_s^n)]\zeta(c_s^n) = \kappa_\Gamma(c_f^m)\zeta(c_f^m)\frac{c_s^2}{2c_f^2}\frac{\left(\frac{1}{c_s^2} - \frac{1}{c_0^2}\right)\left(\frac{1}{c_2} - \frac{1}{c_f}\right)}{\left(\frac{1}{c_f^2} - \frac{1}{c_0^2}\right)\left(\frac{1}{c_s} - \frac{1}{c_2}\right)} \tag{82}$$

$$\alpha^-(c_s^n) = -\kappa_\Gamma(c_f^m)\zeta(c_f^m)\frac{c_s^2}{2c_f^2}\frac{\left(\frac{1}{c_s^2} - \frac{1}{c_0^2}\right)\left(\frac{1}{c_2} - \frac{1}{c_f}\right)\left(\frac{1}{c_s} - \frac{1}{c_f}\right)}{\left(\frac{1}{c_f^2} - \frac{1}{c_0^2}\right)\left(\frac{1}{c_s} + \frac{1}{c_2}\right)\left(\frac{1}{c_s} + \frac{1}{c_f}\right)} \tag{83a}$$

$$\beta^+(c_s^n) = -\kappa_\Gamma(c_f^m)\zeta(c_f^m)\frac{c_s}{4}\frac{\phi}{\left(\frac{1}{c_f^2} - \frac{1}{c_0^2}\right)\left(\frac{1}{c_2} + \frac{1}{c_f}\right)\left(\frac{1}{c_s} + \frac{1}{c_f}\right)} \tag{83b}$$

$$\beta^-(c_s^n) = -\kappa_\Gamma(c_f^m)\zeta(c_f^m)\frac{c_s}{4}\frac{\left(\frac{1}{c_2} - \frac{1}{c_f}\right)\left(\frac{1}{c_s} - \frac{1}{c_f}\right)}{\left(\frac{1}{c_2} + \frac{1}{c_f}\right)} \tag{83c}$$

where

$$\phi = \left(\frac{1}{c_2} + \frac{1}{c_f}\right)\left(\frac{1}{c_s^2} - \frac{1}{c_0^2}\right)\left(\frac{1}{c_f^2} + \frac{1}{c_0^2}\right) + \left(\frac{1}{c_f^2} - \frac{1}{c_0^2}\right)^2\left(\frac{1}{c_2} + \frac{1}{c_f}\right)$$
$$+ \frac{2}{c_f}\left(\frac{1}{c_f^2} - \frac{1}{c_0^2}\right)\left(\frac{1}{c_s^2} + \frac{1}{c_2 c_f}\right) + \frac{2}{c_f}\left(\frac{1}{c_s} + \frac{1}{c_f}\right)\left(\frac{1}{c_2} + \frac{1}{c_f}\right)\left(\frac{1}{c_f c_s} - \frac{1}{c_0^2}\right) \tag{84}$$

c_f and c_s on the right hand sides of equations (82)–(84) are c_f^m and c_s^m, respectively. With the initial values of α^-, β^+ and β^- given by equations (83), the rest of the analysis is similar to the one illustrated in cases II.3 and II.4. The result is as follows. For case III.3, equation (69) determines the unknowns δ and $\kappa_\Gamma(c_f^m)$. For case III.4, equation (71) determines the unknowns $\kappa_\Gamma(c_f^m)$ and $\kappa_\Gamma(c_s^a)$. For the solution to be valid, τ_t^n must be positive, which implies $\kappa_\Gamma(c_f^m) > 0$ by equations (80) and (81). Hence $\beta^+(c_s^n) < 0$ and $\beta^-(c_s^n) < 0$ by equations (83) and $\Omega^n < 0$. By the same argument as in case II.1, $\Omega^a < 0$. Hence σ_t^a as given by equation (69) is indeed between $-\mathbf{t}$ and $\mathbf{s}$, and σ_t^a given by equation (71) is between $-\mathbf{t}$ and $\mathbf{e}_s$.

Group IV

In this group (Figs. 9 and 10), σ^a can be reached from σ^b only through an elastic unloading, an elastic reloading and a plastic loading along the stress path for slow simple waves. There are four cases.

Case IV.1 *and case* IV.2. In these two cases (Fig. 9), the discontinuity in σ is propagated along c_0 with constant strength while the discontinuity in τ is propagated along c_2 with diminishing strength. This is so because c_2 is also the loading boundary c_l.

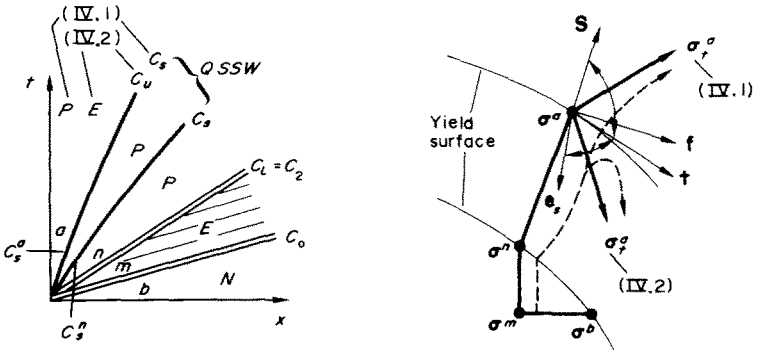

FIG. 9. Cases IV.1 and IV.2.

In the region m, $\mathbf{w}_t^m$ is given by equation (73). Using equation (26) to convert $\mathbf{w}_t^m$ to $\mathbf{w}^{(1)}(\lambda)$ for λ in the region m and let $\lambda = c_2$, we obtain,

$$\mathbf{w}^{m(1)}(c_2) = \left(1 - \frac{c_2}{c_0}\right)\sigma_t^m \begin{bmatrix} -1/\rho c_0 \\ 0 \\ 1 \\ 0 \end{bmatrix}. \tag{85}$$

This is in fact $\mathrm{d}\mathbf{w}/\mathrm{d}t|_{t=0}$ along the lower side of $x = c_2 t$. As to $\mathrm{d}\mathbf{w}/\mathrm{d}t|_{t=0}$ along the upper side of $x = c_2 t$, we have

$$\mathbf{w}^{n(1)}(c_2) = \mathbf{w}^{m(1)}(c_2) + \left(1 - \frac{c_2}{c_0}\right)\sigma_t^m \begin{bmatrix} 0 \\ -\gamma/\rho c_2 \\ 0 \\ \gamma \end{bmatrix} \tag{86}$$

since τ and v alone can be discontinuous across $x = c_2 t$. The fact that c_2 is also the loading boundary means that k should be constant along the upper side of $x = c_2 t$, i.e.

$$\frac{\sigma^n}{\theta^2}\sigma^{n(1)}(c_2)+\tau^n\tau^{n(1)}(c_2) = 0.$$

Using equations (85) and (86), this condition yields

$$\gamma = -\sigma^n/\theta^2\tau^n \tag{87}$$

$\mathbf{w}_t^n$ is now determined by equation (26), i.e.

$$(c_2\mathbf{A}^n-\mathbf{B})\mathbf{w}_t^n = -\mathbf{B}\mathbf{w}^{n(1)}(c_2) \tag{88}$$

and the condition across c_s^n is, by equations (33) and (46),

$$(c_s^n\mathbf{A}^n-\mathbf{B})\mathbf{w}_t^n = -\mathbf{B}\{\alpha^-(c_s^n)\mathbf{r}_{s^-}^n+\beta^+(c_s^n)\mathbf{r}_{f^+}^n+\beta^-(c_s^n)\mathbf{r}_{f^-}^n\}. \tag{89}$$

Omitting the lengthy calculations, we obtain the following result from equations (85)–(89):

$$\alpha^-(c_s^n) = \frac{c_s\left(\frac{1}{c_2}-\frac{1}{c_0}\right)\left(\frac{1}{c_s}-\frac{1}{c_2}\right)\left(\frac{1}{c_s}-\frac{1}{c_0}\right)\left(\frac{1}{c_2^2}-\frac{1}{c_f^2}\right)}{\left(\frac{1}{c_2}+\frac{1}{c_0}\right)\left(\frac{1}{c_s}+\frac{1}{c_2}\right)\left(\frac{1}{c_s^2}-\frac{1}{c_f^2}\right)}\frac{\sigma^n}{\theta^2\tau^n}\sigma_t^m \tag{90a}$$

$$\beta^{\pm}(c_s^n) = \frac{c_f c_s\left(\frac{1}{c_2}-\frac{1}{c_0}\right)\left(\frac{1}{c_2}\pm\frac{1}{c_f}\right)\left(\frac{1}{c_f}\pm\frac{1}{c_0}\right)\left(\frac{1}{c_s^2}-\frac{1}{c_2^2}\right)}{2\left(\frac{1}{c_2}+\frac{1}{c_0}\right)\left(\frac{1}{c_s}\pm\frac{1}{c_f}\right)\left(\frac{1}{c_2}\mp\frac{1}{c_f}\right)}\frac{\sigma^n}{\theta^2\tau^n}\sigma_t^m \tag{90b}$$

where c_f and c_s on the right hand sides of equations (90) are c_f^n and c_s^n, respectively. With the initial values of α^-, β^+ and β^- given by these equations, the rest of the analysis is straight forward. For case IV.1, equation (69) determines the unknowns σ_t^m and ζ while for case IV.2, equation (71) determines the unknowns σ_t^m and $\kappa_\Gamma(c_s^a)$. For the solution to be valid, we must have $\sigma_t^m > 0$. Hence $\beta^{\pm}(c_s^n) > 0$, by equations (90). Thus $\Omega^n > 0$ and $\Omega^a > 0$. Again, this is true in most cases and if this is not the case the discussion at the end of case II.1 applies.

Case IV.3 *and case* IV.4. In these two cases (Fig. 10), the discontinuity in σ is propagated along c_0 while the discontinuity in τ is propagated along c_2, both with constant strength.

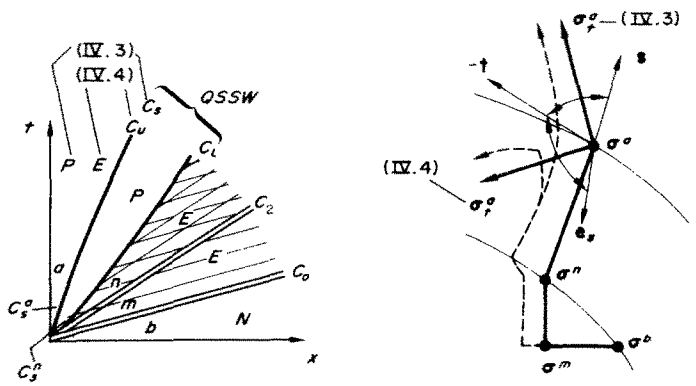

FIG. 10. Cases IV.3 and IV.4.

$\mathbf{w}_t^m$ and $\mathbf{w}_t^n$ are given by equation (73). The condition that the yield stress along c_t should be the same as in the neutral region gives the same equation, equation (75), except all the superscript b should be replaced by n. The rest of the analysis is the same as in cases II.3 and II.4, respectively.

Group V

In this group, $\boldsymbol{\sigma}^a$ can be reached from $\boldsymbol{\sigma}^b$ following the stress path for fast simple waves and then an elastic unloading (Figs. 11 and 12). There are only two cases.

Case V.1. This case applies when $\sigma_t^a < 0$, Fig. 11. $\mathbf{w}_t^m$ is given by equation (57), but since $\sigma_t^m = \sigma_t^a$, we have

$$-\frac{\kappa_\Gamma(c_f^m)\zeta(c_f^m)}{(c_f^m/c_2)^2-1}(\psi_f^m)^2\frac{\theta^2\tau^m}{\sigma^m} = \sigma_t^a. \tag{91}$$

This gives the initial curvature κ_Γ of the unloading boundary. Using equation (91), equation (57) can be written as

$$\mathbf{w}_t^m = \sigma_t^a \begin{bmatrix} -\left(\dfrac{c_f^2}{c_0^2}+1\right)\dfrac{1}{2\rho c_f} \\ -\dfrac{\sigma}{\theta^2\tau}\psi_s^2\left(\dfrac{c_f^2}{c_2^2}+1\right)\dfrac{1}{2\rho c_f} \\ 1 \\ \dfrac{\sigma}{\theta^2\tau}\psi_s^2 \end{bmatrix} \tag{92}$$

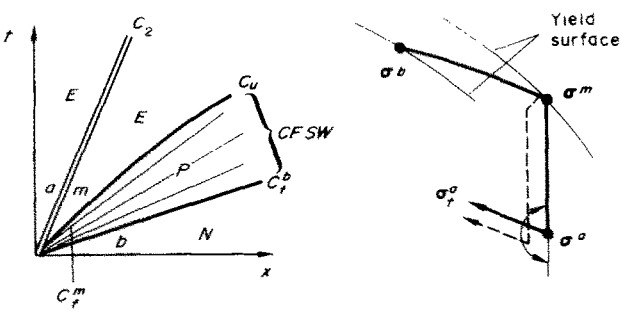

FIG. 11. Case V.1.

where c_f, ψ_s, σ and τ are c_f^m, ψ_s^m, σ^m and τ^m, respectively. The discontinuity in τ and v are propagated with constant strength along $x = c_2 t$. As in case I.4, the unloading boundary c_u and the solution in the elastic region bounded by c_2 and c_u depend only on the boundary value $\sigma(0, t)$ and are independent of $\tau(0, t)$.

Case V.2. This case applies when $\sigma_t^a > 0$, Fig. 12. The region m is a region of fast simple waves, and hence,

$$\mathbf{w}_t^m = \gamma \mathbf{r}_f^m. \tag{93}$$

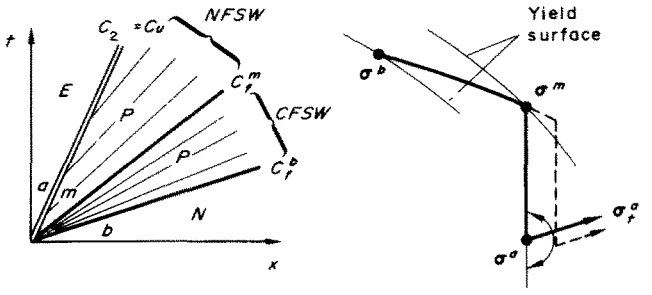

FIG. 12. Case V.2.

Since c_2 is also an unloading boundary, the discontinuities in τ and v are propagated along $x = c_2 t$ with varying strength. Across $x = c_2 t$, we have

$$\tau^e - \tau^p = -\rho c_2 (v^e - v^p).$$

Along the upper side of $x = c_2 t$, we have

$$\tau^e - \rho c_2 v^e = \text{const.}$$

Hence

$$\frac{d\tau^e}{dt} = \frac{1}{2}\frac{d\tau^p}{dt} + \rho c_2 \frac{dv^p}{dt} \tag{94a}$$

$$\frac{dv^e}{dt} = \frac{1}{\rho c_2}\frac{d\tau^e}{dt}. \tag{94b}$$

If we use equation (26) to convert $\mathbf{w}_t^m$ expressed by equation (93) into $\mathbf{w}^{m(1)}(c_2)$ we obtain

$$\mathbf{w}^{m(1)}(c_2) = \gamma\left(1 - \frac{c_2}{c_f^m}\right)\mathbf{r}_f^m. \tag{95}$$

Noticing that $\mathbf{w}^{m(1)}(c_2) = d\mathbf{w}^p/dt$ and $\mathbf{w}^{a(1)}(c_2) = d\mathbf{w}^e/dt$ in this case, we obtain from equations (94) and (95),

$$\mathbf{w}^{a(1)}(c_2) = \gamma\left(1 - \frac{c_2}{c_f}\right)\begin{bmatrix} \psi_f/\rho c_f \\ -\left(1 - \frac{c_2}{c_f}\right)\Big/ 2\rho c_2 \\ -\psi_f \\ -\left(1 - \frac{c_2}{c_f}\right)\Big/ 2 \end{bmatrix}. \tag{96}$$

If we use equation (26) again to convert $\mathbf{w}^{a(1)}(c_2)$ into $\mathbf{w}_t^a$, we obtain

$$\gamma = \frac{\left(\frac{1}{c_2^2} - \frac{1}{c_0^2}\right)\left(\frac{1}{c_f^2} - \frac{1}{c_0^2}\right)}{\left(\frac{1}{c_2^2} - \frac{1}{c_f^2}\right)^2}\frac{\theta^2 \tau^a}{\sigma^a}\sigma_t^a. \tag{97}$$

In equations (96) and (97), c_f and ψ_f are c_f^m and ψ_f^m, respectively. Since $\sigma_t^a > 0$, $\gamma > 0$. The solution is valid. As in the previous case the solution in the region of *NFSW* depends only on $\sigma(0, t)$, not on $\tau(0, \tau)$.

Group VI

In this group, $\boldsymbol{\sigma}^a$ is located inside the yield surface which passes through $\boldsymbol{\sigma}^b$, and is to the left of $\boldsymbol{\sigma}^b$. The solution is trivial. If $\sigma(0, t) = g(t)$ and $\tau(0, t) = h(t)$, we have

$$\sigma(x, t) = g\left(t - \frac{x}{c_0}\right), \qquad \tau(x, t) = h\left(t - \frac{x}{c_2}\right). \tag{98}$$

Thus, we have an elastic simple wave solution.

7. DISCUSSION AND CONCLUDING REMARKS

The solutions presented in the preceding section are for a thin-walled tube, which is initially prestressed beyond the elastic limit, subjected to a discontinuous loading at the boundary $x = 0$. The discontinuity occurs at $t = 0$, and after $t = 0$ the loads at $x = 0$ are arbitrary but continuous. If the initially prestressed state is not in the plastic region, the solutions obtained in the last section are modified by adding an elastic shock wave of constant magnitude along $x = c_0 t$. For any given discontinuous loading condition, a solution exists and is unique, except the unlikely case in which Ω^a of equation (70) vanishes. The question whether Ω^a can be zero or not is still open, mathematically at least, since this amounts to finding $\mathbf{w}^{(1)}(\lambda)$ of equation (21) analytically. Physically, $\Omega^a = 0$ does not seem to represent a realistic situation.

From the results obtained, it is seen that a discontinuous jump from a lower yield surface to a higher yield surface, and a continuous loading into an even higher yield surface thereafter at the boundary $x = 0$, does not necessarily produce a continuous plastic flow for other sections near the boundary of the tube. This phenomenon is not unexpected in view of the previous studies on the same problem with less general boundary conditions [2, 4]. There are, however, other results which are new and unexpected. For instance, the dependence of the solution and the elastic–plastic boundary on $\sigma(0, t)$ alone, not on $\tau(0, t)$ prescribed at the boundary as discussed in cases I.4, V.1 and V.2, is unexpected. As is well-known, the solution is in general dependent on the boundary conditions $\sigma(0, t)$ and $\tau(0, t)$. Another unexpected result is the coincidence of the elastic–plastic boundary with the shear wave front c_2 as discussed in cases IV.1, IV.2 and V.2.

The continuity of the solutions from one case to the other within a group is obviously satisfied. Less obvious is the continuity of the solutions from one group to the other group. As we stated in the beginning of Section 6, groups I and II are particular cases of other groups but since the results are not readily reducible, they are presented as separate groups. To illustrate this point, let us consider case III.2, Fig. 7, in which $\boldsymbol{\sigma}^a$ is very close to $\boldsymbol{\sigma}^m$. In the limiting case when $\boldsymbol{\sigma}^a = \boldsymbol{\sigma}^m$, case III.2 should be reduced to case I.2, Fig. 2. Thus case I.2 is a particular case of case III.2. But in the particular case I.2, we need to determine the initial speed of the unloading boundary c_u, which is given by equation (55), while for the general case III.2 the initial c_u is c_s^a. This sounds like a contradiction but a look at Fig. 13 explains the paradox. Figure 13 shows qualitatively the wave pattern in the $x \sim t$ plane of case III.2 when $\boldsymbol{\sigma}^a$ is very close to $\boldsymbol{\sigma}^m$. The region of $QSSW$ will be very small and vanishes when $\boldsymbol{\sigma}^a = \boldsymbol{\sigma}^m$.

Another example is the particular case of case III.4, Fig. 8, when $\boldsymbol{\sigma}^b$ is very close to $\boldsymbol{\sigma}^m$. In the limit when $\boldsymbol{\sigma}^b = \boldsymbol{\sigma}^m$ we should obtain case II.4, Fig. 6. Figure 14 shows qualitatively how case III.4 is reduced to case II.4 as $\boldsymbol{\sigma}^b$ approaches $\boldsymbol{\sigma}^m$. In the limit, the region of $CFSW$

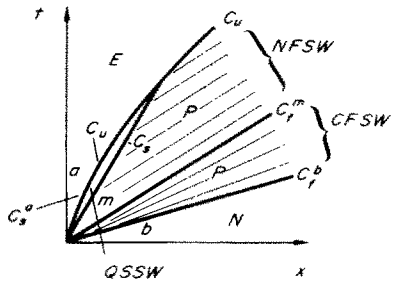

FIG. 13. Case III.2 with $\sigma^a \cong \sigma^m$. This is reduced to case I.2 when $\sigma^a = \sigma^m$.

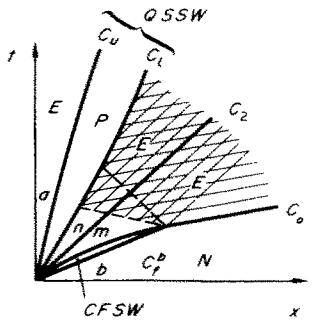

FIG. 14. Case III.4 with $\sigma^b \cong \sigma^m$. This is reduced to case II.4 when $\sigma^b = \sigma^m$.

disappears. The thin lines in the elastic regions indicate that the solutions there are simple wave solutions. Notice that the precursor wave, or the wave front, in the neutral region is propagated first at the constant speed of c_f^b, and then c_0. This is unusual in view of the fact that the material is assumed to be homogeneous and the yield stress in the neutral region is constant in this example.

Two more examples of limiting process are depicted in Figs. 15 and 16. In both figures, the discontinuity in shear across c_2 diminishes to zero at some distance from the origin. In Fig. 15, the distance at which the discontinuity vanishes depends on how close σ^b is to σ^n. In Fig. 16, this depends on how close σ^a is to σ^m. Both figures are self-explanatory.

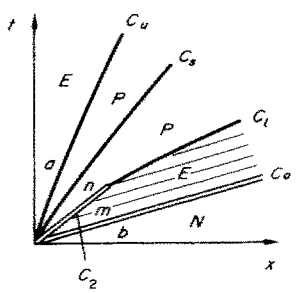

FIG. 15. Case IV.2 with $\sigma^b \cong \sigma^n$. This is reduced to case II.2 when $\sigma^b = \sigma^n$

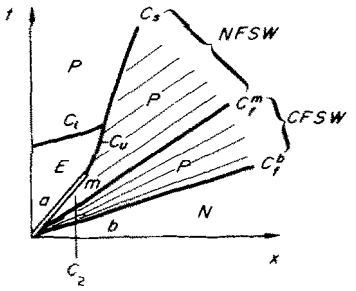

FIG. 16. Case V.2 when $\sigma^a \cong \sigma^m$ and $k_t^a > 0$. This is reduced to case I.1 when $\sigma^a = \sigma^m$.

It should be emphasized from these examples that the solutions obtained in Section 6 apply only to the neighborhood of the origin $x = 0$, $t = 0$.

The analysis presented here can be applied to the case where σ^b and σ^a are not in the same quadrant in the $\sigma \sim \tau$ plane. It can also be applied to the case where $\sigma(0, t)$ for $t < 0$ is not necessarily constant, i.e. $\sigma_t^b \neq 0$. The results presented in Sections 4 and 5 are fairly general and can be applied to other types of combined stress waves such as pressure-two-shear waves [10] and to other types of materials such as combined isotropic and kinematic work hardening materials [11] subject to impact loadings.

REFERENCES

[1] KH. A. RAKHMATULIN, On the propagation of waves of unloading. *Prikl. Mat. Mekh.* **9**, 91–100 (1945).
[2] R. J. CLIFTON, An Analysis of Combined Longitudinal and Torsional Plastic Waves in a Thin-Walled Tube, *Proceedings of the 5th U.S. National Congress of Applied Mechanics*, ASME, pp. 465–480 (1966).
[3] T. C. T. TING, Elastic–plastic boundaries in the propagation of plane and cylindrical waves of combined stress. *Q. appl. Math.* **4**, 441–449 (1970).
[4] T. C. T. TING, On the initial slope of elastic–plastic boundaries in combined longitudinal and torsional wave propagation. *J. appl. Mech.* **36**, 203–211 (1969).
[5] A. JEFFREY and T. TANIUTTI, *Nonlinear Wave Propagation with Applications to Physics and Magnetohydrodynamics*. Academic Press (1964).
[6] R. COURANT and D. HILBERT, *Methods of Mathematical Physics*, Vol. II. Interscience (1962).
[7] F. B. HILDERBRAND, *Methods of Applied Mathematics*. Prentice-Hall (1952).
[8] P. D. LAX, Hyperbolic systems of conservation laws II. *Communs pure appl. Math.* **10**, 537–566 (1957).
[9] R. J. CLIFTON, Elastic–plastic boundary in combined longitudinal and torsional plastic wave propagation. *J. appl. Mech.* **35**, 782–786 (1968).
[10] R. P. GOEL and L. E. MALVERN, Elastic–plastic plane waves with combined compressive and two shear stresses in a half-space. *J. appl. Mech.* to appear.
[11] R. P. GOEL and L. E. MALVERN, Biaxial plastic simple waves with combined kinematic and isotropic hardening. *J. appl. Mech.* **37**, 1100–1106 (1970).
[12] R. J. CLIFTON and S. R. BODNER, An analysis of longitudinal elastic-plastic pulse propagation. *J. appl. Mech*, **33**, 248–255 (1966).

(*Received* 3 *May* 1971; *revised* 16 *June* 1971)

Абстракт—Цаются решение в момент конца удара по тонкостенной трубе, край готорой $x=0$ предварительно напряжен и подвержен действию разривной, сложной, продольной и крутильной нагрузок, для времени $t=0$. Подразумевается, что нагрузка для $x=0$ после $t=0$ изменяется постоянно. Получается решение для всех возможных комбинаций разрывных нагрузок для $t=0$ и для всех возможных комбинаций нагрузок после $t=0$. Цаются: характеристики решений в каждом районе трубы, начальная скороств и иногда начальное ускорение на границы между двумя районами. Все они оказываются полезными указателями для полного решения слжного распространения волны напряжения в тонкостенной трубе, подверженной действию нагрузки произвольного удара.